Mobile Netw Appl (2012) 17:90–99
DOI 10.1007/s11036-010-0281-3

# Mobility-Assisted Node Localization Based on TOA Measurements Without Time Synchronization in Wireless Sensor Networks

**Hongyang Chen · Bin Liu · Pei Huang · Junli Liang · Yu Gu**

Published online: 1 December 2010


**Abstract** Wireless sensor networks (WSNs) have been proposed for a multitude of location-dependent applications. To stamp the collected data and facilitate communication protocols, it is necessary to identify the location of each sensor. In this paper, we discuss the performance of two novel positioning schemes, which use two generalized geometrical localization algorithms to achieve an accurate estimation based on time-of-arrival (TOA) measurements without time synchronization. In order to improve the network performance and address the limitations of static WSNs on position estimation, a mobile anchor is utilized effectively and two attractive movement strategies for mobile anchor are designed accordingly. The effectiveness of our approaches is validated and compared with the traditional Trilateration method by extensive simulations.

**Keywords** TOA · geometrical location · wireless sensor networks

H. Chen (✉)
Institute of Industrial Science, The University of Tokyo, Tokyo, Japan
e-mail: hongyang@mcl.iis.u-tokyo.ac.jp

B. Liu
Computer Science Department, University of Southern California, Los Angeles, CA, USA

P. Huang
Department of Computer Science and Engineering, Michigan State University, East Lansing, MI, USA

J. Liang
School of Automation and Information Engineering, Xi'an University of Technology, Xi'an, China

Y. Gu
Information Systems Architecture Science Research Division, National Institute of Informatics, Tokyo, Japan

## 1 Introduction

Recent advances in wireless communications and micro electro-mechanical system (MEMS) technologies have enabled the development of low-cost, low-power and small size wireless sensor nodes [19]. Wireless sensor networks (WSNs) have become the current hot spot of networking area and have been used for various applications, such as oceanic resource exploration, pollution monitoring, tsunami warnings and mine reconnaissance. For all these applications, it is essential to know the locations of the data [37].

Many approaches to obtain this per-node location knowledge have been explored. Based on the type of knowledge used in localization, we can divide these localization protocols into two categories: range-based and range-free [30]. Range-based protocols estimate absolute point-to-point distance to calculate the location between neighboring sensors. The second classes of methods, named range-free approach, employ connectivity or other features to find the connections from the non-anchor nodes to the anchor nodes [1, 12]. Range-based algorithms are typically based on angle-of-arrival (AOA), RSSI [23, 28], time-of-arrival (TOA) or time-difference-of-arrival (TDOA) measurements [2, 21, 34]. A promising technology is the ultra wideband (UWB) technology where precise ranging can be embedded into data communication. The typical range-

free localization algorithms include DV-Hop [18], Centroid algorithm [25], APIT [12] and Amorphous [13]. However, the performance of range-free algorithms is not high. When the sensor network is anisotropic or has complex topology, the performance of these methods also tends to deteriorate. Because the location accuracy of the range-based approach is relatively higher than that of range-free algorithms, we focus on the study of range-based solutions and their applications in WSNs in this paper. Received signal strength is comparatively much easier and less costly to obtain from the time series recordings at each sensor. However, the accuracy for the RSSI-based algorithm is not high. It is our opinion that the TOA based localization can play an active role in several WSNs applications provided that the accuracy requirement in terms of spatial resolution is strict. As such, we propose two TOA based localization algorithms and evaluate them when applied to mobility-assisted wireless sensor networks. Unlike the static sensors, which are tightly constrained by the energy supplies, mobile anchor's batteries are rechargeable. Efficient collaboration between mobile anchor (MA) and static sensors can also effectively change anchor densities on demand, potentially reducing the number of anchors needed comparing to all-static network deployments. Furthermore, mobile anchors can cooperate with the static sensors to fix the limitation of node localization in the static sensor networks. In this paper, mobile anchor node roams through the network and broadcasts beacon messages with its position to unknown-position nodes periodically at various locations. Based on the active movement of mobile anchor, localization performance is improved significantly.

This paper makes the following two main contributions. First, two previous localization algorithms based on the area and volume are generalized to allow any number of MA beacon points, which were inspired by the area method used in [28] and the volume method utilized in [29], respectively. Second, two attractive movement strategies for MA are proposed to reduce the total moving distance and improve moving efficiency of MA while satisfying the expected location performance, which can efficiently extend the lifetime of the MA and optimize the anchor distribution.

The rest of this paper is organized as follows. Section 2 introduces the related works. Section 3 provides the derivation of the proposed localization algorithm. Section 4 gives the analysis of the communication cost and energy consumption. In Section 5, simulation results are shown, some considerations about the impact of (additive white gauss noise) AWGN and Rayleigh fading are discussed. Finally, we present our conclusions in Section 6.

## 2 Related Works

Recent work demonstrated that the sensing performance of WSNs can be improved by using mobility capability node. Xing et al. [35] study target detection for mobility-assisted WSNs. They exploited reactive mobility to improve the target detection performance of WSNs. In their approach, mobile sensors collaborate with static sensors and move reactively to achieve the required detection performance. Wang et al. [32] used Voronoi diagrams to detect the coverage holes and devised three movement-assisted sensor deployment protocols based on the principle of moving sensors from densely deployed areas to sparsely deployed areas. Wang et al. [31] presented a mobility-assisted network for field coverage which can be remarkably improved by integrating a small set of mobile sensors. They offered an optimal algorithm to calculate the coverage contributions, which explores the potentials of the mobile sensors and extends the network lifetime.

Several studies exploited the effect of mobile nodes on node localization for WSNs. In these methods, a small number of mobile devices referred to as MAs roam about sensing fields and assist to improve localization performance. Luo et al. [15] proposed a TDOA localization algorithm for movement-assisted sensor networks. A mobile beacon is used to measure the mobility-differentiated TOA in [15], which will increase mobile beacon's communication cost. Based on the RF-based technology, [36] presented three algorithms for tracking transceiver-free moving objects in an indoor WSN.

RSSI has been widely used as a distance measure in the context of static WSNs because of its simplicity. The impact of a number of parameters, such as the operating frequency, the transmitter–receiver distance, the variation of transceivers, the antenna orientation, and the environment, on (received signal strength) RSS measurements were investigated using Tmote Sky nodes in real outdoor environments [25]. The results in [17] describe a thorough empirical study of the RSS in Mica2 sensor node for indoor environments with considering parameters such as operating frequency, antenna orientation, battery voltage, temporal and spatial properties of environment, and the environmental dynamics. Lymberopoulos et al. [16] investigated the RSS variability in 3-D indoor environment. In their experiments, all the sensor nodes are equipped with Chipcon CC2420 radio with monopole antennas. Their study is mainly focusing on the impact of the antenna orientation over the RSS.

Complementary to the above studies that deal with the node localization based on RSS measurements, we

focus on improving target localization performance by utilizing the mobility of sensors. Different with the former work, our method takes advantage of mobility-assisted WSNs which can efficiently detect the obstacle in the communication range and decrease the effect of non-line of sight (NLOS) through the active movement of MA. Since the MA is often resource rich node attached with better processing ability and longer transmission range comparing to the static sensor node, a series of beacon messages with its position will be broadcasted by the MA in our localization scheme, which will reduce the communication cost of static sensors. Thus, the unknown-position nodes will actively capture TOA measurements and initiate localization algorithm after receiving the incoming data from the MAs. The positions of MAs are known since they are usually equipped with GPS receivers or RFID tags [35], which will be acted as mobile anchor nodes in our localization system. If obstacles exist in between a sensor and certain anchors, static node might not obtain enough and accurate TOA measurements to estimate its position. Different from prior studies, we exploit mobile sensors as anchors for localization and thus avoids the deployment of a large number of static anchors. By including a MA to replace multiple static anchors, we avoid the above disadvantage of static WSNs. Comparing with previous work, our algorithm dose not require the time synchronization between MA and unknown-position sensors. However, several challenges must be fixed in order to make best use of the mobility of WSNs in target estimation. First, considering the higher design complexity and manufacturing cost, the number of mobile anchors available in a network is often limited. Therefore, MAs must effectively cooperate with static sensors to obtain the maximum utility. Second, the moving trace of MAs must be optimized since MAs are only capable of low-speed and short-distance mobility in real environment due to the high power consumption of locomotion [9, 24]. The efficient moving scheme for MAs can further increase location accuracy for target estimation since the distribution of anchors can affect location performance in the static WSNs. In our algorithm, interesting moving trace is designed to improve the localization performance.

## 3 Algorithm Development

In mobility-assisted WSNs, depending on some emergent applications there may be a need to rapidly respond to sensor input [10]. For instance, in a fire application, actions should be performed on the event area as soon as possible. Moreover, the collected and delivered sensor data must still be valid at the time of acting. Different with former work on node localization for WSNs, the MA movement and coordination play an important role to provide accurate and timely localization to sensors. We will devise an attractive movement strategy for MAs to address this problem later.

The network proposed in this paper consists of static sensor nodes, which are located randomly, and MAs, which have a priori knowledge of their own positions with respect to a global coordinate system.

In our localization mechanism, the distance between target node and MA is observable using the TOA measurement. The procedure for our scheme to obtain TOA measurements works as follows: the MA periodically transmits a beacon signal to unknown-position sensor nodes in range. During this period, sensor nodes will constantly calculate the TOA measurement from each MA beacon point orderly and store them for later use. The detailed ranging scheme is given as the following subsection.

### 3.1 TOA Measurements Based Ranging Without Time Synchronization

Let $P$ be an arbitrary unknown-position ordinary node. MA stops at a certain position. As shown in Fig. 1, the basic ranging scheme takes two steps.

In the first step, MA broadcasts a ranging request which can be heard by all the ordinary nodes in range. Then in the second step, each ordinary node sends an ACK to MA to response the request. Note that the ordinary nodes need conduct a backoff before sending the ACK to prevent the potential collisions at MA. Taking $P$ as an example, it is clear that we have

$$\begin{cases} d_{MA,P} = c\,(T_{P1} - T_{A1}) \\ d_{P,MA} = c\,(T_{A2} - T_{P2}) \end{cases} \Rightarrow d_{MA,P} = \frac{c}{2}\,[(T_{A2} - T_{A1}) - (T_{P2} - T_{P1})] \quad (1)$$

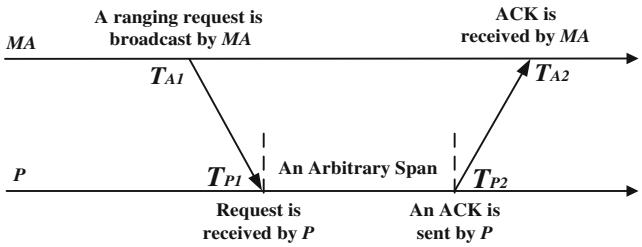


**Fig. 1** Basic ranging scheme

where $c$ is the speed of light. Obviously, since $T_{A2} - T_{A1}$ and $T_{P2} - T_{P1}$ are the elapsed times at MA and $P$ respectively; they can be calculated by using the local clocks of MA and $P$. Therefore, no time synchronization between MA and $P$ is required. In addition, although the backoff span is uncertain, it does not affect the performance of our ranging scheme.

### 3.2 Mathematical Procedure for Two-Dimensional Geometrical Localization

In [28], Wan et al. proposed a localization algorithm using trilinear coordinates. However, their method considers only three base stations and it is not feasible when there are more than three anchors in range for an unknown-position sensor. In this subsection, we extend their method to the scenario of two-dimensional sensor networks.

Let $M(x_0, y_0)$ be the target node location and $(X_i, Y_i)$ be the known location of the $i$'th beacon points from MA. For instance, unknown-position node randomly selects three beacon points in range, which can construct a triangle $ABC$.

Any three numbers proportional to the directed distances from $M$ to the sidelines $BC$, $CA$, $AB$, in that order, are called *trilinear coordinates* for $M$. Given triangle $ABC$, the *trilinear coordinates* of a point $M$ with respect to the triangle is denoted as $(\alpha, \beta, \gamma)$, which is proportional to the corresponding algebraic distances of $M$ from the sidelines of the triangle, e.g. $BC$, $CA$, $AB$. By *algebraic*, that $\alpha$ has to be taken positive if $M$ and $A$ lie on the same side of $BC$ and negative in the contrary. Analogous the conventions for the signs of $\beta$ and $\gamma$. We then have [28]

$$\begin{aligned}
\Delta &= \sqrt{s\,(s-a)\,(s-b)\,(s-c)} \\
\Delta 1 &= \sqrt{s1\,(s1-a)\,(s1-r2)\,(s1-r3)} \\
\Delta 2 &= \sqrt{s2\,(s2-b)\,(s2-r1)\,(s2-r3)} \\
\Delta 3 &= \sqrt{s3\,(s3-c)\,(s3-r1)\,(s3-r2)}
\end{aligned} \tag{2}$$

and

$$\begin{aligned}
s &= (a+b+c)/2 \\
s1 &= (a+r2+r3)/2 \\
s2 &= (b+r1+r3)/2 \\
s3 &= (c+r1+r2)/2
\end{aligned} \tag{3}$$

where $\Delta$, $\Delta 1$, $\Delta 2$, $\Delta 3$ are the areas of $\Delta ABC$, $\Delta MBC$, $\Delta MCA$, $\Delta MAB$ and $a$, $b$, and $c$ are the lengths of triangle $ABC$ sides. $ri$ is the distance between the $i$'th anchor node and the source node, where $i = 1, 2, 3$.

The relationship between the area and the *trilinear coordinates* is given by [28]:

$$\alpha a + \beta b + \gamma c = 2\Delta. \tag{4}$$

Straight-line equations for sides of the triangle, e.g. $BC$, $CA$, $AB$, are defined as [28]

$$y_0 = k_i x_0 + d_i \tag{5}$$

Then the equations of parallel lines $BC$, $CA$, $AB$ through point $M$ are defined as [28]:

$$\begin{aligned}
y_0 &= k_1 x_0 + d_1 + \alpha\sqrt{1+k_1^2} \\
y_0 &= k_2 x_0 + d_2 + \beta\sqrt{1+k_2^2} \\
y_0 &= k_3 x_0 + d_3 + \gamma\sqrt{1+k_3^2}
\end{aligned} \tag{6}$$

Obviously, the intersection of these parallel lines will close to the real position of target sensor node.

Since $\Delta 1$, $\Delta 2$, $\Delta 3$ are all related to $M(x_0, y_0)$, we convert Eq. 6 into

$$h_c = G_c Z_c \tag{7}$$

where $Z_c = [x_0, y_0]^T$ and $h_c = \begin{bmatrix} k_1 & -1 \\ k_2 & -1 \\ k_3 & -1 \end{bmatrix}$,

$$G_c = \begin{bmatrix} -d_1 - \alpha\sqrt{1+k_1^2} \\ -d_2 - \beta\sqrt{1+k_2^2} \\ -d_3 - \gamma\sqrt{1+k_3^2} \end{bmatrix}.$$

Using Least Square (LS) algorithm, we get [14]

$$Z_c = G_c^{-1} h_c. \tag{8}$$

Then the estimate of $M(x_0, y_0)$ using these three beacon points is expressed as $x_0 = Z_c(1)$ and $y_0 = Z_c(2)$.

Furthermore, the unknown-position node can select all possible combination of three beacon points from all of that of MA points in range. The final position estimate for unknown-position sensor node is the average of all $Z_c$ values.

### 3.3 Mathematical Procedure for Three-Dimensional Geometrical Localization

Wan et al. [29] proposed a localization algorithm for mobile system based on a linear relationship between the rectangular and the volume coordinates. However, only four (base station) BSs can be utilized in [29]. Inspired by the volume method utilized in [29], we develop a new volume based localization approach which allows any number of MA beacon points. The proposed generalized geometrical location algorithm is based on

the volume of the tetrahedron which is formed by the target senor node and MA.

In this section, we generalize the volume based localization approach in [29] with any number of anchor nodes. The linear relationship between the rectangular and the volume coordinates can be found in [29]. The detailed derivation procedure for our generalized volume based localization method will be described in this subsection.

**Lemma 1** *Assume that the rectangular coordinate of the vertex $A_i$ of the tetrahedron is $(x_i, y_i, z_i), i = 1, 2, 3, 4$. Then its signed volume can be expressed in the form of determinant as follows* [29]*:*

$$V = \frac{1}{6}\begin{vmatrix} 1 & 1 & 1 & 1 \\ x_1 & x_2 & x_3 & x_4 \\ y_1 & y_2 & y_3 & y_4 \\ z_1 & z_2 & z_3 & z_4 \end{vmatrix} = \frac{1}{6}\begin{vmatrix} x_2 - x_1 & y_2 - y_1 & z_2 - z_1 \\ x_3 - x_2 & y_3 - y_2 & z_3 - z_2 \\ x_4 - x_3 & y_4 - y_3 & z_4 - z_3 \end{vmatrix} \quad (9)$$

**Lemma 2** *The volume of the general tetrahedron is also given by the determinant* [29]

$$V^2 = \frac{1}{288}\begin{vmatrix} 0 & 1 & 1 & 1 & 1 \\ 1 & 0 & r_{12}^2 & r_{13}^2 & r_{14}^2 \\ 1 & r_{12}^2 & 0 & r_{23}^2 & r_{24}^2 \\ 1 & r_{13}^2 & r_{23}^2 & 0 & r_{34}^2 \\ 1 & r_{14}^2 & r_{24}^2 & r_{34}^2 & 0 \end{vmatrix} \quad (10)$$

*where $r_{ij}$ is the range between vertexes $A_i$ and $A_j$.*

Let $A = \begin{bmatrix} 1 & 1 & 1 & 1 \\ X_1 & X_2 & X_3 & X_4 \\ Y_1 & Y_2 & Y_3 & Y_4 \\ Z_1 & Z_2 & Z_3 & Z_4 \end{bmatrix}$ and $P(x_0, y_0, z_0)$ be the random unknown-position node location and $(X_i, Y_i, Z_i)$ be the known location of the $i$th MA beacon point. The four MA beacon points $A_1$, $A_2$, $A_3$, $A_4$ will be used to calculate the position of target node. The MA beacon points $A_1$, $A_2$, $A_3$, $A_4$ and unknown-position sensor can form tetrahedrons. Then using Lemma 1 we can get the volume coordinates of the unknown node $P(v_{1i}, v_{2i}, v_{3i}, v_{4i})$.

As shown in Eqs. 1–3 of [29] , only four MA beacon points in range can be used for unknown-position sensor nodes positioning. In order to use any number of beacon points in range, we generalize their scheme as follows.

Using Eqs. 1–3 of [29], we obtain

$$v_{1i} = \frac{1}{6}\begin{vmatrix} 1 & 1 & 1 & 1 \\ x_0 & X_2 & X_3 & X_i \\ y_0 & Y_2 & Y_3 & Y_i \\ z_0 & Z_2 & Z_3 & Z_i \end{vmatrix} \quad (11)$$

$$v_{2i} = \frac{1}{6}\begin{vmatrix} 1 & 1 & 1 & 1 \\ X_1 & x_0 & X_3 & X_i \\ Y_1 & y_0 & Y_3 & Y_i \\ Z_1 & z_0 & Z_3 & Z_i \end{vmatrix} \quad (12)$$

$$v_{3i} = \frac{1}{6}\begin{vmatrix} 1 & 1 & 1 & 1 \\ X_1 & X_2 & x_0 & X_i \\ Y_1 & Y_2 & y_0 & Y_i \\ Z_1 & Z_2 & z_0 & Z_i \end{vmatrix} \quad (13)$$

$$v_{4i} = \frac{1}{6}\begin{vmatrix} 1 & 1 & 1 & 1 \\ X_1 & X_2 & X_3 & x_0 \\ Y_1 & Y_2 & Y_3 & y_0 \\ Z_1 & Z_2 & Z_3 & z_0 \end{vmatrix} \quad (14)$$

where $i \geq 4$.

Let $A_i = \begin{bmatrix} 1 & 1 & 1 & 1 \\ X_1 & X_2 & X_3 & X_i \\ Y_1 & Y_2 & Y_3 & Y_i \\ Z_1 & Z_2 & Z_3 & Z_i \end{bmatrix}$, $V_i = \frac{1}{6}\begin{vmatrix} 1 & 1 & 1 & 1 \\ X_1 & X_2 & X_3 & X_i \\ Y_1 & Y_2 & Y_3 & Y_i \\ Z_1 & Z_2 & Z_3 & Z_i \end{vmatrix}$, $i \geq 4$. From Eqs. 11–14, we get $\begin{bmatrix} v_{14} \\ v_{24} \\ v_{34} \\ v_{44} \end{bmatrix} = \frac{1}{6}A_4^* \begin{bmatrix} 1 \\ x_0 \\ y_0 \\ z_0 \end{bmatrix}$,

$\begin{bmatrix} v_{15} \\ v_{25} \\ v_{35} \\ v_{45} \end{bmatrix} = \frac{1}{6}A_5^* \begin{bmatrix} 1 \\ x_0 \\ y_0 \\ z_0 \end{bmatrix}$, and

$$\begin{bmatrix} v_{1i} \\ v_{2i} \\ v_{3i} \\ v_{4i} \end{bmatrix} = \frac{1}{6}A_i^* \begin{bmatrix} 1 \\ x_0 \\ y_0 \\ z_0 \end{bmatrix} \quad (15)$$

where $A_i^*$ is the adjugate matrix of the matrix $A_i$.

Let $T = \begin{bmatrix} 1 \\ x_0 \\ y_0 \\ z_0 \end{bmatrix}$. Using Eq. 15, we have

$$\begin{bmatrix} v_{14} & v_{15} & \cdots & v_{1i} \\ v_{24} & v_{25} & \cdots & v_{2i} \\ v_{34} & v_{35} & \cdots & v_{3i} \\ v_{44} & v_{45} & \cdots & v_{4i} \end{bmatrix} = \frac{1}{6}\left[ \mathrm{A}_4^* \ \mathrm{A}_5^* \cdots \mathrm{A}_i^* \right] \begin{bmatrix} T \\ T \\ \vdots \\ T \end{bmatrix} \quad (16)$$

Then Eq. 16 can be converted into

$$h_{cv} = G_{cv} Z_{cv} \quad (17)$$

where $Z_{cv} = [\,T\ T \cdots T\,]^T$, $h_{cv} = \begin{bmatrix} v_{14} & v_{15} & \cdots & v_{1i} \\ v_{24} & v_{25} & \cdots & v_{2i} \\ v_{34} & v_{35} & \cdots & v_{3i} \\ v_{44} & v_{45} & \cdots & v_{4i} \end{bmatrix}$,

$G_{cv} = \frac{1}{6}\left[\,A_4^*\ A_5^* \cdots A_i^*\,\right]$.

Using least square (LS) algorithm [14], we get

$$Z_{cv} = (G_{cv}^T G_{cv})^{-1} G_{cv}^T h_{cv} \tag{18}$$

Then the position of target node $P(x_0, y_0, z_0)$ is expressed as $x_0 = Z_{cv}(2)$, $y_0 = Z_{cv}(3)$, and $z_0 = Z_{cv}(4)$.

### 3.4 Movement Strategy for Mobile Anchors

Due to the power constraint, MA is only capable of low-speed and short-distance movement in real deployments. For instance, the normal speed of several mobile sensor platforms (e.g., Packbot and XYZ) is only 0.5∼2m/s. A XYZ mobile sensor node can move only about 165 m before exhausting its power, which is supported by two AA batteries [35]. Therefore, the movement trace of MA must be efficiently planned in order to maximize the amount of target positions that can be obtained with satisfied localization accuracy within a short moving distance. Moreover, scheduling an optimal path for MA improves the system reliability and network lifetime [3, 4, 6–8, 27–29].

To address the above constraints, we propose an efficient moving trace for MAs. We use a 'S' type as macro moving trace for MA illustrated in Fig. 2. The target area can be divided into small circulars developed by MA's different positions. The radius of the circular is dependent on radio range of MA. In practical environment, the radio pattern is not a theoretical circular model because of degree of irregularity for radio signal. Here, we use circular model only for simple presentation. As shown in Fig. 2, for micro-moving pattern, the MA starts to move from c0 and

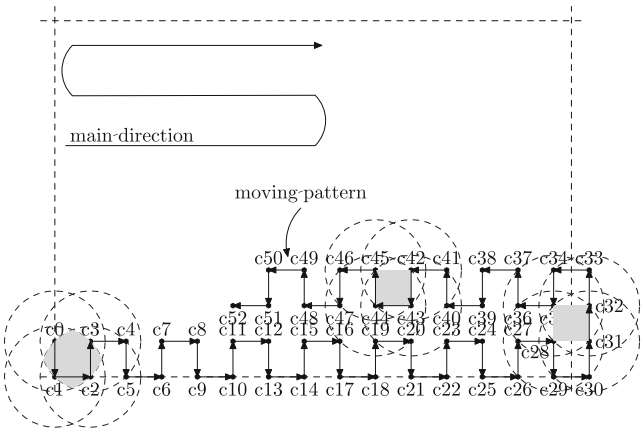


**Fig. 2** Movement strategy

intermittently stops at c1 after moving $R/\sqrt{2}$, where $R$ is the radio range of MA. When MA stops at c1, it broadcasts a beacon message including its position to other sensor nodes in its radio range. After a short stop, MA continues to move as the same way. Note that although we can utilize any number of MA beacon points as proposed in the previous subsection, we use only four optimal beacon points in a cell coverage area to reduce the cost for MA. Based on this attractive moving strategy, unnecessary movement of MA is avoided, MA can effectively decrease the total moving distance and number of broadcast to extend its lifetime and improve the system reliability. Another merit for this moving strategy, the unknown nodes can receive four uniformly distributed beacon messages in one little square area, which can increase location accuracy.

#### *3.4.1 Effective Side for the Cell Coverage Area*

We regard those little rectangles as the effective coverage areas. In order to make the best use of MA, we need to assure all of the unknown-position nodes can receive the beacon messages from MA. Thus, we let $c_0c_2 = R$. Let the side of little rectangles be $e$ and $f$, respectively. In order to maximum the use of MA, we need to find a rectangle which has the maximize area but the minimum perimeter. We define $\lambda$ to be the ratio between the area and perimeter for the little rectangle. Thus, we get:

$$\lambda = \frac{ef}{2(e+f)} = \frac{1}{2(1/e+1/f)} \le \frac{1}{4(ef)^{-1/2}}. \tag{19}$$

Consequently, we obtain the maximum value of $\lambda$, $\lambda_{\max} = \frac{\sqrt{2}R}{8}$, when $e = f = R/\sqrt{2}$. Thus, the optimal cell coverage area for our localization scheme is square.

#### *3.4.2 Efficient Moving Trace for Emergent Environment*

In some emergent environments, such as fire alarm, mobile anchor should move into this area and find the position of source of fire as soon as possible. To address the above constraints, we propose an efficient moving trace for MA. We use a spiral movement as macro moving trace for MA illustrated in Fig. 3, which is inspired from the biological behavior. The target area can be divided into small circulars developed by MA's different positions. The radius of the circular is dependent on radio range of MA. In practical environment, the radio pattern is not a theory circular model with the effect of degree of irregularity. Here, we use the circular model only for simple presentation. As shown in Fig. 3 for micro-moving pattern, the MA starts to move from c0

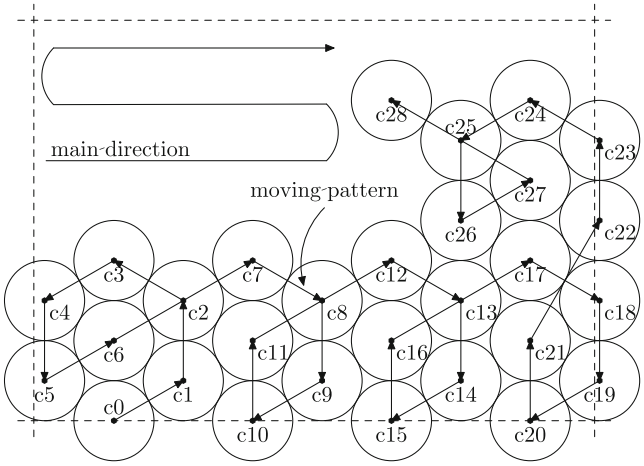


**Fig. 3** Movement strategy

and intermittenly stops at c1 after moving $2R$. When MA stops at c1, it can detect and receive the event information from other sensor nodes in its radio range. After a short stop, MA continues to move as the same way and stops at c2. Based on this attractive moving strategy, unnecessary movement of MA is avoided. MA can effectively detect the emergent event and calculate the position from the emergent sensing event. The main merit for this moving strategy is that it is very efficient to capture the emergency event information and find the position of related sensor nodes with short time since the spiral type macro moving trace can cover the largest application area in a short time.

Based on this moving strategy, unnecessary movements of MA are avoided. It can effectively decrease the total moving distance and number of broadcast to extend the MA's lifetime and improve the system reliability.

## 4 Communication Cost and Power Consumption

The number of messages that a sensor node needs to transmit is treated as the communication cost in our localization algorithm. In our localization process, the MAs will perform the broadcasting operation at every time slot. Thus the communication cost is related to the number of beacon signals, which can be calculated as follows:

For the communication cost in the 'S' type, we need to utilize those square areas as the effective coverage area to take best advantage of MAs. Since $c_0c_2 = R$, we have $2q^2 = R^2$, where $q$ represents the side of little squares. As a result, $q = R/\sqrt{2}$. Note that $c_2c_3c_4c_5$ can be constructed by $c_0c_1c_2c_3$ and $c_4c_5c_6c_7$. Thus, let $l$ be the width of the deployment area, the number of useful little squares in a row can be calculated as $l/2q = l/\sqrt{2}R$. In the same way, let $h$ be the height of deployment area, the number of rows is $h/2q = h/\sqrt{2}R$. For each useful little square, MA will beacon four times. Therefore, the total number of beacons is $4(hl)/(2R^2) = 2hl/R^2$. The MA broadcasts to unknown-position sensors a hello message with its ID, location and some recognize-bits which amounts to only several bytes. For low beacon point density, this would require roughly hundreds of bytes.

We can evaluate the corresponding energy consumption of the 'S' type approach. We account for the energy consumed in locomotion of the MA, wireless communication, and idle state at local sensors. We assume that the MA is a wheeled robot such as the Robomote [11]. The energy consumed in locomotion by a wheeled robot, denoted by $E_M(d)$, can be approximated by $E_M(d) = k \bullet d$ [33], where $d$ is the moving distance and $k = 2\,\mathrm{J/m}$ if the MA moves at an optimal speed. For typical low-power transceivers such as CC2420, the energy consumed in wireless communication, denoted by $E_C(d)$, can be modeled as $E_C(d) = m \bullet (a + b \bullet d^2)$ [22], where $d$ is the transmission distance, $m$ is the number of bits transmitted, and $a$ and $b$ are constants. $a$ and $b$ can be set to be $0.6 \times 10^{-7}\,\mathrm{J/bit}$ and $4 \times 10^{-10}\,\mathrm{J/m^2} \bullet$ bit according to the experiments in [22]. The power consumption of an idle node is set to be 21 mW, which is consistent with that of the TelosB mote [26]. We assume that a node stays asleep when it is outside of the communication range of the MA during the localization phase. Moreover, we ignore the power consumption of a sleeping node, as it is much less than the idle state power consumption. For instance, a TelosB mote consumes 1 μW in sleep mode [26].

In our 'S' type case, the energy consumed in wireless communication by the MA is $E_c(R) = m \bullet (a + b \bullet R^2) \bullet \frac{2hl}{R^2}(J)$, the energy consumed in locomotion by the MA is $E_m(d) = \frac{\sqrt{2}hl}{R}(J)$, and the average power consumption of sensors in the MA radio coverage area is $E_s = 21 \bullet N_s(mW)$, where $N_s$ is the average number of sensors in the MA radio coverage. Therefore, $N_s = \rho \bullet \pi R^2 = \frac{N\pi R^2}{A}$, where $N$ is the total number of sensors and $A$ is the total area of the network.

## 5 Simulation Results and Discussions

### 5.1 Simulation Results for Two-Dimensional Localization

In this section, simulation results are presented and analyzed. We deploy 100 sensor nodes randomly in

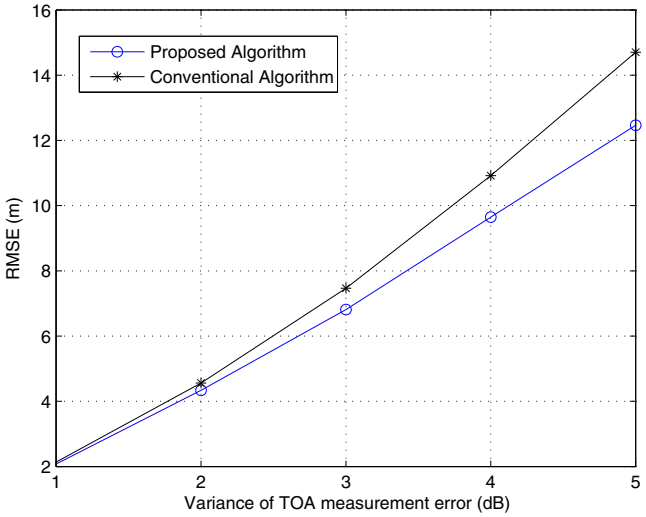


**Fig. 4** Position errors of algorithm in LOS environment

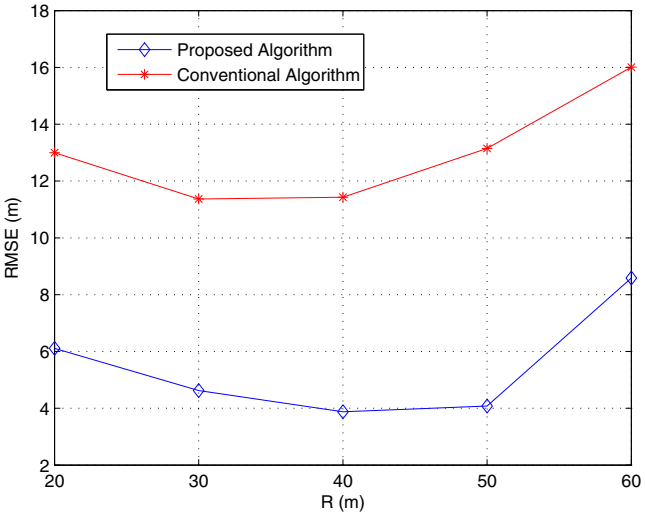


**Fig. 6** Position errors of algorithm in AWGN Channels

a two-dimensional space. The radio range of sensor nodes (R) is set to 50 m first. We simulated a single general node with four different positions of MA beacons in a cell coverage area, and explored single point estimation through sets of 1,000 independent simulations. Each run generated a given number of different positions of MA beacon points randomly. The TOA measurement error caused by target node and all network devices is assumed to be Gaussian distributed with mean 0 and variance $1 * i$ dB (where $i = 1, 2, \ldots, 5$ [20]. Secondly, we simulate our algorithm based on AWGN and Rayleigh channels respectively [14]. For AWGN and Rayleigh channels, extra noises are added to the simulation accordingly. Root-mean-square error (RMSE) is calculated to evaluate the performance of localization algorithms. Matlab is used as a simulation tool. Simulation results are presented in the Figs. 4, 5, 6 and 7.

As can be seen from the simulation results of Fig. 4, our proposed algorithm achieves better performance than the Trilateration algorithm [13] in line-of-sight (LOS) environment. The RMSE increases as the measurement error variance increases. From Fig. 4, we can see that the RMSE of our scheme is smaller than that of the conventional TOA algorithm using Trilateration. Figure 5 is the cumulative density function of position error. Over 99% of the nodes have less than 5 m error in our proposed algorithm, but it decreases to 91% for the conventional TOA algorithm using Trilateration. For the same variance, position error is smaller when our scheme is applied in LOS environ-

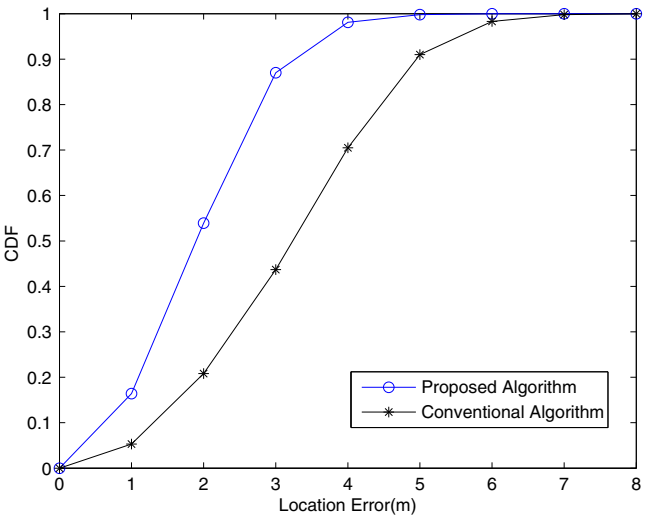


**Fig. 5** Cumulative distribution functions of estimation error

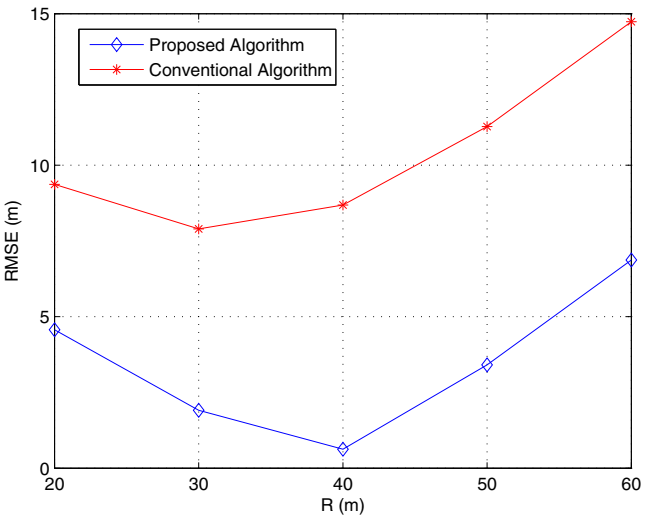


**Fig. 7** Position errors of algorithm in Rayleigh Channels

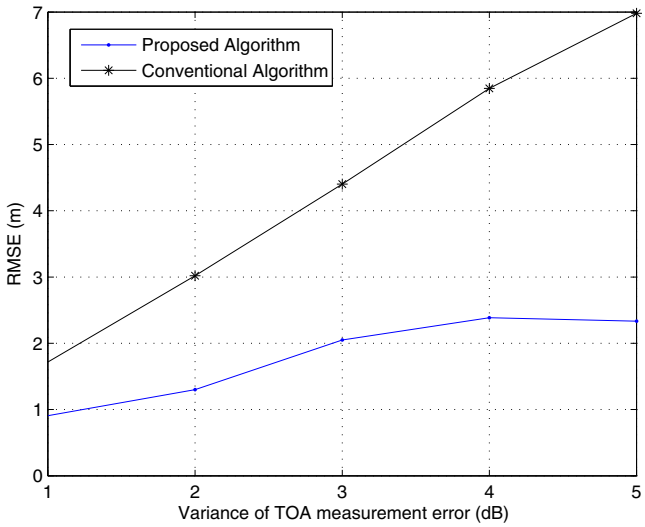


**Fig. 8** Position errors of algorithm in LOS environment

ment than in AWGN or Rayleigh channels as shown in Figs. 6 and 7. In AWGN and Rayleigh channels, our proposed algorithm also behaves better than the conventional TOA algorithm in this scenario. Hence, the performance of our scheme exceeds the conventional TOA location algorithm using Trilateration from our simulation results.

### 5.2 Simulation Results for Three-Dimensional Localization

In this section, simulation results are presented and analyzed. The simulation parameters are same as the previous subsection. Simulation results are presented in Figs. 8 and 9.

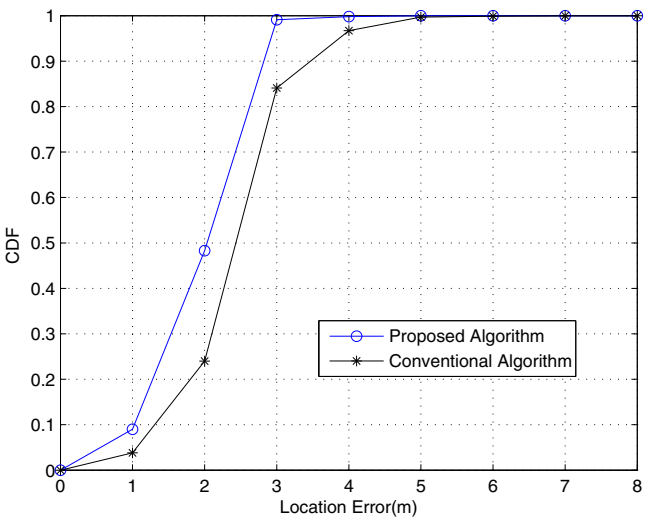


**Fig. 9** Cumulative distribution functions of estimation error

As can be seen from the simulation results of Fig. 8, our proposed algorithm still achieves better performance than the conventional TOA algorithm using Trilateration in 3D LOS environment. From Fig. 8, we can also see that the RMSE of our scheme is smaller than that of the conventional TOA algorithm using Trilateration in this scenario. Figure 9 is the cumulative density function of the position error. Over 99% of the nodes have less than 4m error in our proposed algorithm, but it decreases to 96% for the conventional TOA algorithm. The performance of our volume-based localization scheme exceeds the conventional TOA location algorithm from our simulation results in three-dimensional WSN.

## 6 Conclusions and Future Work

In the paper, we have proposed two schemes for node localization which use the generalized geometrical location algorithms to achieve more accurate estimation in mobility-assisted wireless sensor networks. Our positioning schemes do not require sensor nodes to make radio transmission constantly but listen to MA beacon signals passively. This efficiently reduces sensor energy cost and also improves the usage ratio of RF channels. Two effective moving traces for MA are devised to make best use of MA while achieving the localization requirement. As shown in the simulation results, it is found that the proposed approaches are effective and have good location accuracy than that of the conventional Trilateration algorithm. In the future, we will implement our algorithms via real testbeds to verify their performances.

**Acknowledgements** The authors would like to thank the anonymous reviewers for their helpful and constructive comments. Part of this work was presented at IEEE ICPADS'08 [5].

## References

1. Bulusu N, Heidemann J, Estrin D (2000) GPS-less low cost outdoor localization for very small devices. IEEE Pers Commun Mag 7(5):28–34
2. Chen H, Deng P, Xu Y, Li X (2005) A robust location algorithm with biased extended kalman filtering of TDOA data for wireless sensor networks. In: Proc. IEEE international conference on wireless communications, networking and mobile computing (WCNM 2005). Wuhan, China, pp 883–886
3. Chen H, Deng P, Xu Y, Li X (2006) A novel localization scheme based on RSS data for wireless sensor networks. In: Proc. APWeb workshops 2006, pp 315–320
4. Chen H, Huang P, So HC, Luo X, Deng P (2008) Mobility-assisted cooperative localization scheme for wireless sen-

sor networks. In: Proc. military communications conference (MILCOM 2008). San Diego, USA, pp 1–7
5. Chen H, Huang P, So HC, Sezaki K (2008) Mobility-assisted position estimation in wireless sensor networks. In: Proc. 14th IEEE international conference on parallel and distributed systems (ICPADS 2008). Melbourne, Victoria, Australia, pp 607–614
6. Chen M, Gonzalez S, Leung VCM (2007) Applications and design issues of mobile agents in wireless sensor networks. IEEE Wirel Commun Mag 14(6):20–26
7. Chen M, Kwon T, Choi Y (2006) EDDD: energy-efficient differentiated directed diffusion (EDDD) for real-time traffic in wireless sensor networks. Comput Commun (Elsevier) 29(2):231–245
8. Chen M, Kwon T, Yuan Y, Choi Y, Leung VCM (2007) MADD: mobile-agent-based directed diffusion in wireless sensor networks. EURASIP J Appl Signal Process 2007(1):219–242
9. Chen M, Leung V, Mao S (2009) Directional controlled fusion in wireless sensor networks. Mobile Netw Appl (ACM/Springer) 14(2):220–229
10. Chen M, Leung V, Mao S, Xiao Y, Chlamtac I (2009) Hybrid geographical routing for flexible energy-delay trade-offs. IEEE Trans Veh Technol 58(9):4976–4988
11. Dantu K, Rahimi M, Shah H, Babel S, Dhariwal A, Sukhatme GS (2005) Robomote: enabling mobility in sensor networks. In: Proc. int. symp. on information processing in sensor networks (IPSN). Los Angeles, CA, pp 404–409
12. He T, Huang C, Blum BM, Stankovic JA, Abdelzaher TF (2003) Range-free localization schemes in large scale sensor networks. In: Proceedings of ACM MobiCom, pp 81–95
13. Hoene C, Willmann J (2008) Four-way TOA and software-based trilateration of IEEE 802.11 devices. In: Proc. PIMRC2008. Cannes, France, pp 1–6
14. Kay SM (1993) Fundamentals of statistical signal processing: estimation theory. Prentice-Hall, Englewood Cliffs
15. Luo J, Shukla HV, Hubaux JP (2005) Non-interactive location surveying for sensor networks with mobility-differentiated ToA. In: Proceedings of the 24th annual conference of the IEEE communications societies (INFOCOM'05). Miami, Florida, USA, pp 1–12
16. Lymberopoulos D, Lindsey Q, Savvides A (2006) An empirical analysis of radio signal strength variability in IEEE 802.15.4 networks using monopole antennas. ENALAB technical report 050501, EWSN 2006
17. Ma J, Chen Q, Zhang D, Ni LM (2006) An empirical study of radio signal strength in sensor networks in using MICA2 nodes. Technical report, HKUST
18. Niculescu D, Nath B (2001) Ad-hoc positioning system. In: Proceeding of IEEE global communications conference (GLOBECOM 2001), pp 2926–2931
19. Ou CH, Ssu KF (2008) Sensor position determination with flying anchors in three-dimensional wireless sensor networks. IEEE Trans Mobile Comput 7(9):1084–1097
20. Patwari N, Hero AO, Perkins M, Correal N, Dea RJO' (2003) Relative location estimation in wireless sensor networks. IEEE Trans Signal Process 51(8):2137–2148
21. Rappapport TS (1996) Wireless communications: principles and practice. Prentice Hall, New Jersey, pp 50–143
22. Sha M, Xing G, Zhou G, Liu S, Wang X (2009) C-MAC: modeldriven concurrent medium access control for wireless sensor networks. In: Proc. INFOCOM. Rio de Janeiro, Brazil, pp 1845–1853
23. Shi Q, He C, Chen H, Jiang L (2010) Distributed wireless sensor network localization via sequential greedy optimization algorithm. IEEE Trans Signal Process 58(6):3328–3340
24. Spyropoulos T, Rais R, Turletti T, Obraczka K, Vasilakos AV (2010) Routing for disruption tolerant networks: taxonomy and Design. Wirel Netw (ACM/Springer) 16(8):2349–2370
25. Stoyanova T, Kerasiotis F, Prayati A, Papadopoulos G (2007) Evaluation of impact factors on RSS accuracy for localization and tracking applications. In: Proc. MobiWac'07. Chania, Crete Island, Greece, pp 9–16
26. TelosB datasheet, Crossbow Technology Inc
27. Venkatesh S, Buehrer RM (2007) Non-line-of-sight identification in ultra-wideband systems based on received signal statistics. IET Microwaves, Antennas & Propagation 1(6):1120–1130
28. Wan Q, Liu S, Peng YN (2002) Source location method based on corrected trilinear coordinates. Acta Electronica Sinica 30(2):843–845. In Chinese
29. Wan Q, Peng YN (2002) An improved 3-dimensional mobile location method using volume measurements of tetrahedron. IEICE Trans Commun E85-B:1817–1823
30. Wang C, Chen J, Sun Y (2010) Sensor network localization using kernel spectral regression. Wireless Commun Mobile Comput 10(8):1045–1054
31. Wang D, Liu J, Zhang Q (2007) Mobility-assisted sensor networking for field coverage. In: Proceeding of IEEE global communications conference (GLOBECOM 2007), pp 1190–1194
32. Wang G, Cao G, Porta TL (2004) Movement-assisted sensor deployment. In: Proc. IEEE INFOCOM 2004, pp 2469–2479
33. Wang G, Irwin MJ, Berman P, Fu H, La Porta TF (2005) Optimizing sensor movement planning for energy efficiency. In: Proc. of international symposium on low power electronics and design (IPSLED). San Francisco, CA, pp 215–220
34. Whitehouse K, Culler D (2002) Calibration as parameter estimation in sensor networks. In: Proceedings of ACM international workshop on wireless sensor networks and application, pp 59–67
35. Xing G, Wang J, Shen K, Huang Q, Jia X, So HC (2008) Mobility-assisted spatiotemporal detection in wireless sensor networks. In: Proc. 28th international conference on distributed computing systems (ICDCS), Beijing, China, June 17–20, 2008, pp 103–110
36. Zhang D, Ma J, Chen Q, Ni LM (2007) An RF-based system for tracking transceiver-free objects. In: Proc. fifth annual IEEE international conference on pervasive computing and communications, 2007 (PerCom '07), pp 135–144
37. Zhong Z, He T (2009) Achieving range-free localization beyond connectivity. In: Proc. ACM SenSys'09. Berkeley, CA, pp 281–294